

# Optical spectral imaging of degeneration of articular cartilage

## Jussi Kinnunen

University of Eastern Finland  
Department of Physics and Mathematics  
P.O.B. 111  
FI-80101, Joensuu, Finland

## Jukka S. Jurvelin

University of Eastern Finland  
Department of Physics and Mathematics  
P.O.B. 1627  
FI-70211, Kuopio, Finland

## Markku Hauta-Kasari

University of Eastern Finland  
School of Computing  
P.O.B. 111  
FI-80101, Joensuu, Finland

## Pasi Vahimaa

University of Eastern Finland  
Department of Physics and Mathematics  
P.O.B. 111  
FI-80101, Joensuu, Finland

## Simo Saarakkala

University of Eastern Finland  
Department of Physics and Mathematics  
P.O.B. 1627  
FI-70211, Kuopio, Finland

## 1 Introduction

Osteoarthritis (OA), the most common joint disease, is characterized by the degenerative changes in articular cartilage. Depletion of superficial proteoglycans,<sup>1-5</sup> changes in collagen fibril orientation,<sup>3,4,6,7</sup> and reduction in the collagen content<sup>4</sup> are early signs of OA. Later, they lead to an increase of articular surface roughness<sup>8</sup> and debilitate the mechanical integrity of articular cartilage by decreasing its stiffness.<sup>9,10</sup> Frequently, as a complement to x-ray imaging, OA can be clinically diagnosed by arthroscopic examination.

In OA, visual color changes of the articular cartilage surface can be observed during arthroscopy, i.e., the loss of glister and the change from white color to more yellowish. Furthermore, when evaluating the healing of the cartilage repair tissue after surgical repair procedures, similar color changes are observed.<sup>11,12</sup> These changes are visually and subjectively assessed through an arthroscope, and typically they can be clearly observed only when present in more advanced stages of OA. Consequently, there is a need for more quantitative

**Abstract.** Osteoarthritis (OA) is a common musculoskeletal disorder often diagnosed during arthroscopy. In OA, visual color changes of the articular cartilage surface are typically observed. We demonstrate *in vitro* the potential of visible light spectral imaging (420 to 720 nm) to quantificate these color changes. Intact bovine articular cartilage samples ( $n=26$ ) are degraded both enzymatically using the collagenase and mechanically using the emery paper (P60 grit, 269  $\mu\text{m}$  particle size). Spectral images are analyzed by using standard CIELAB color coordinates and the principal component analysis (PCA). After collagenase digestion, changes in the CIELAB coordinates and projection of the spectra to PCA eigenvector are statistically significant ( $p<0.05$ ). After mechanical degradation, the grinding tracks could not be visualized in the *RGB* presentation, i.e., in the visual appearance of the sample to the naked eye under the D65 illumination. However, after projecting to the chosen eigenvector, the grinding tracks are revealed. The tracks are also seen by using only one wavelength, i.e., 469 nm, however, the contrast in the projection image is 1.6 to 2.5 times higher. Our results support the idea that the spectral imaging can be used for evaluation of the integrity of the cartilage surface. © 2010 Society of Photo-Optical Instrumentation Engineers. [DOI: 10.1117/1.3477190]

Keywords: optical reflectance; articular cartilage; color; spectral imaging; principal component analysis.

Paper 09482RR received Nov. 3, 2009; revised manuscript received Jun. 24, 2010; accepted for publication Jun. 24, 2010; published online Aug. 13, 2010.

and accurate methods for diagnostic purposes.

Optical spectral assessment was applied earlier for bovine hip joint,<sup>13</sup> rabbit cartilage plugs after osteochondral autografting,<sup>11</sup> rabbit cartilage after microfracture repair,<sup>12</sup> and human articular cartilage.<sup>14</sup> The studies have found color coordinate changes in the CIELAB colorimetric system when the cartilage integrity changes.<sup>11,12,14</sup> A model for the reflectance spectrum as a function of the cartilage thickness has also been proposed.<sup>13</sup> Further optical properties, such as scattering and absorption coefficients and anisotropy, within the whole visible range of the spectrum have been reported for cartilage tissue.<sup>15,16</sup> Based on those studies, cartilage has been found to be highly forward-scattering tissue. However, in these earlier studies only a small area on the cartilage surface was analyzed. Thus, spatial spectroscopic assessment of the cartilage surface has not been conducted. Further, all of the earlier studies have been limited to very simple spectral analysis methods. With more sophisticated analysis methods, it may be possible to extract more detailed information on the integrity of the cartilage.

The main aim of this *in vitro* study was to investigate the

Address all correspondence to: Jussi Kinnunen, University of Eastern Finland, Department of Physics and Mathematics, P.O.B. 111, FI-80101, Joensuu, Finland. Tel: 358-13-25-17-919. E-mail: jussi.kinnunen@uef.fi

effect of superficial degeneration on the optical spectrum of bovine articular cartilage. Controlled tissue degeneration was artificially created with enzymatic digestion using collagenase enzyme and mechanical grinding with an emery paper (P60). In addition to the color coordinate changes, the changes in the reflectance spectrum of cartilage before and after experimental procedures were analyzed with sophisticated spectral analysis methods, such as principal component analysis (PCA). Further, as a second aim we clarified the differences of the spectra between the patellar and femoral bovine cartilage.

## 2 Materials and Methods

### 2.1 Articular Cartilage Samples and Experimental Degradations

Bovine knee joints were obtained from the local abattoir (Atria Oyj, Kuopio, Finland). Joints were opened and cylindrical osteochondral samples ( $n=32$ , diameter=19 mm) were prepared from the lateral upper quadrant of patella (PAT,  $n=26$ ) and from the femoral medial condyle (FMC,  $n=6$ ). All samples were visually intact except one: the patella with a spontaneous cartilage degeneration, probably associated with an earlier trauma, was also included in the study as a purpose of comparison with the artificial degradations. After preparation, the samples were kept in phosphate-buffered saline (PBS) until degradative treatments.

In enzymatic degradation, collagenase enzyme (111 U/ml, Collagenase Type 1a, C9891, Sigma Aldrich, St. Louis, Missouri) was used with different incubation times to obtain variable stages of degeneration. From PAT samples 8 were incubated for 6 h, and 11 PAT samples and 6 FMC samples were incubated for 15 h. Furthermore, 7 samples from the patella were exposed to mechanical grinding of the surface with an emery paper (P60 grit, 269  $\mu\text{m}$  particle size, KWH Mirka Ltd, Finland). The grinding was performed manually by sliding the cartilage surface two times against the emery paper. The slides were approximately at a 90-deg angle. The spectral images were collected for all samples before and after experimental treatments.

### 2.2 Acquisition of Spectral Data

The spectral images were captured by using the Nuance liquid crystal tunable filter (LCTF) spectral camera (model N-MSI-420-10, Cambridge Research & Instrumentation, Woburn, Massachusetts) (Fig. 1). The used spectral range of the camera was 420 to 720 nm with 7-nm sampling. The measurements were conducted in standard 45/0 measurement geometry (45 illumination angle, normal detection angle). To simulate the arthroscopic evaluation, the samples were immersed in PBS during measurements. Illumination was by a 50-W halogen light (Accentline 50W GU5.3 12V 36D 1CT, Koninklijke Philips Electronics N.V., Amsterdam, Netherlands) driven by a mixed-mode-regulated precision laboratory power supply (EX1810R, Thurlby Thandar Instruments Ltd., Huntingdon, United Kingdom) and detection of the sample was made through a glass window of the custom-made sample container. Spectral data with the dynamic of 12 bits was acquired using optimal integration times for each measured channel with the camera software (Nuance 1.6.8.2), and the data were further analyzed with a custom-made MATLAB program (Math-

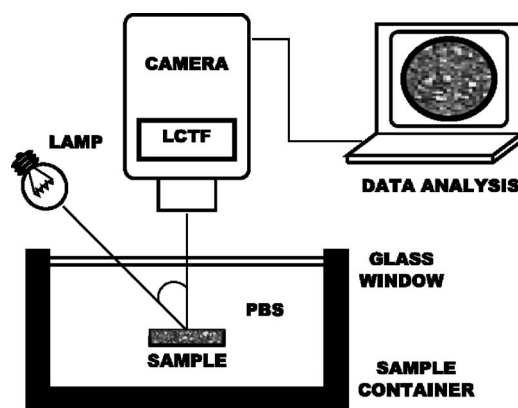


**Fig. 1** Schematic presentation of the measurement setup as viewed from top. Measurements were conducted through a glass window with an LCTF camera in 45/0 geometry while the sample was immersed in PBS.

Works, Inc., Natick, Massachusetts). In the imaging system, the visible area was 14 mm in diameter corresponding to 850 pixels in the image, which resulted in a pixel resolution of the data to be 60.7 pixels/mm. The spatial resolution of 14.25 lp/mm was assessed by using a USAF-1951 (U.S. Air Force 1951) resolution target (RES-2, Newport Corporation, Fountain Valley, California).

### 2.3 Spectral Analysis

The acquired reflectance spectral images were analyzed using PCA. In addition, the spectral data were transformed into CIELAB uniform color space.<sup>17</sup> The reflectance  $R(\lambda)$  of the sample at each pixel of the spectral image was calculated using

$$R(\lambda) = \frac{I_{\text{sample}}(\lambda) - I_{\text{dark}}(\lambda)}{I_{\text{reference}}(\lambda) - I_{\text{dark}}(\lambda)}, \quad (1)$$

where  $I_{\text{sample}}$  is spectral power distribution of the illumination reflected from the sample,  $I_{\text{reference}}$  is spectral power distribution of the illumination reflected from the perfectly reflecting diffuser, and  $I_{\text{dark}}$  is the detector dark signal. The  $I_{\text{reference}}$  was measured using an optical polytetrafluoroethylene (PTFE) reference material (ODM98, Gigahertz-Optik GmbH, Germany) with uniform 98% diffuse reflectance over the visible range. The reference material with a size equal to that of the tissue samples was placed in the system, and the  $I_{\text{reference}}$  was measured using individually optimized integration times for each wavelength channel. The reference material was replaced with the cartilage sample, and the  $I_{\text{sample}}$  was measured by using the same integration times. The  $I_{\text{dark}}$ , with corresponding integration times, was measured to reduce the effect of any stray light and camera bias.

The PCA for a set of spectra  $\mathbf{R}$  from the  $x \times y \times n$  spectral image

$$\mathbf{R} = \begin{bmatrix} R_{11}(\lambda_1) & \cdots & R_{xy}(\lambda_1) \\ \vdots & \ddots & \vdots \\ R_{11}(\lambda_n) & \cdots & R_{xy}(\lambda_n) \end{bmatrix}, \quad (2)$$

where  $n$  is the number of the wavelengths, and  $x \times y$  is the number of pixels, can be calculated as follows. The  $n \times n$  correlation matrix  $\mathbf{C}$  of the data is defined as

$$\mathbf{C} = \frac{1}{x \times y} \mathbf{R} \mathbf{R}^T. \quad (3)$$

Eigenvectors  $\Phi$  of  $\mathbf{C}$  are solutions of the equation

$$\mathbf{C}\Phi = \sigma\Phi, \quad (4)$$

where  $\sigma$  is the diagonal matrix of  $\mathbf{C}$ 's eigenvalues. The eigenvectors form an orthonormal basis in the function space of measured spectra. These vectors are organized so that the one corresponding to highest eigenvalue is the first and so forth. The original image can be reconstructed accurately by a linear combination of those vectors.<sup>18</sup> In this study, the characteristics of the data were studied by calculating projections of spectra to the eigenvectors of correlation matrix.

The CIELAB color coordinates ( $L^*a^*b^*$ ) can be calculated from the spectra by using the Commission internationale de l'éclairage (CIE) standard observer and any chosen illumination.<sup>17</sup> The D65 standard daylight and CIE1931 standard observer were used in this study. First, the projections of the measured spectrum to the XYZ color-matching functions were calculated as follows.

$$X = k \sum_{\lambda} S(\lambda) R(\lambda) \bar{x}(\lambda) \Delta\lambda, \quad (5)$$

$$Y = k \sum_{\lambda} S(\lambda) R(\lambda) \bar{y}(\lambda) \Delta\lambda, \quad (6)$$

$$Z = k \sum_{\lambda} S(\lambda) R(\lambda) \bar{z}(\lambda) \Delta\lambda, \quad (7)$$

where  $S(\lambda)$  is the spectral power distribution of the chosen illumination; and  $\bar{x}(\lambda)$ ,  $\bar{y}(\lambda)$ , and  $\bar{z}(\lambda)$  are the color-matching functions of the standard observer. The  $Y$  has a value of 100 for the perfectly reflecting diffuser when the scaling factor  $k$  is defined as

$$k = \frac{100}{\sum_{\lambda} S(\lambda) \bar{y}(\lambda)}. \quad (8)$$

The nonlinear transformation from the XYZ coordinate system to the CIELAB system is defined using the following equations:<sup>17</sup>

$$L^* = \begin{cases} 116 \left( \frac{Y}{Y_n} \right)^{1/3} - 16 & \text{if } \frac{Y}{Y_n} > 0.008856 \\ 903.3 \left( \frac{Y}{Y_n} \right) & \text{if } \frac{Y}{Y_n} \leq 0.008856 \end{cases}, \quad (9)$$

$$a^* = 500 \left[ \left( \frac{X}{X_n} \right)^{1/3} - \left( \frac{Y}{Y_n} \right)^{1/3} \right], \quad (10)$$

$$b^* = 200 \left[ \left( \frac{Y}{Y_n} \right)^{1/3} - \left( \frac{Z}{Z_n} \right)^{1/3} \right], \quad (11)$$

where  $X_n$ ,  $Y_n$ , and  $Z_n$  denote the tristimulus values of the illumination. Equations (10) and (11) are valid when  $X/X_n$ ,  $Y/Y_n$ , and  $Z/Z_n$  are all greater than 0.008856. Otherwise the cube root in the equation in question [Eq. (10) or Eq. (11)] is replaced by

$$\left( \frac{a}{a_n} \right)^{1/3} \rightarrow \left[ 7.787 \left( \frac{a}{a_n} \right) + 16/116 \right], \quad (12)$$

where  $a$  is either  $X$ ,  $Y$ , or  $Z$ .<sup>17</sup>

The  $L^*$  denotes the brightness of the color. Coordinate  $a^*$  denotes the blueness ( $a^* > 0$ ) or the yellowness ( $a^* < 0$ ), and the  $b^*$  coordinate denotes the redness ( $b^* > 0$ ) or the greenness ( $b^* < 0$ ) of the color. In the CIELAB system, the color difference  $\Delta E_{ab}^*$  is almost uniform for all color pairs and is defined as the Euclidean distance between the coordinates:<sup>17</sup>

$$\Delta E_{ab}^* = [(\Delta L^*)^2 + (\Delta a^*)^2 + (\Delta b^*)^2]^{1/2}. \quad (13)$$

## 2.4 Contrast Evaluation

The contrast  $C$  between the grinding tracks and the intact areas for the mechanically degenerated cartilage was evaluated by using the Michelson contrast equation:

$$C = \frac{\max(I) - \min(I)}{\max(I) + \min(I)}, \quad (14)$$

where  $I$  is the value of a pixel in a chosen pair of pixels. Totally 60 pairs of pixels, one pixel with clearly visible grinding tracks and another with intact cartilage nearby, were selected from each sample image. The pixels were selected as sparsely as possible to reduce the global variation, and a  $5 \times 5$ -pixel window within the selected pixels was used for the contrast evaluation to reduce the local variations. The derived 60 values were averaged to represent the contrast of the grinding tracks for the specific sample.

## 2.5 Optical Microscopy

After the optical reflectance measurements, one representative sample from each sample group was processed for histological evaluation with an optical microscope (Axio Imager M2, Zeiss, Germany). Histological 3- $\mu\text{m}$ -thick sections were prepared and stained with 0.5% safranin-O as described earlier.<sup>19</sup> The sections were imaged and the integrity of the articular surface and proteoglycan content of the samples were visually evaluated. For each sample, cartilage thickness was also determined from the captured images, calibrated by using a 1-mm ruler.

## 2.6 Statistical Analysis

The nonparametric Wilcoxon signed rank test was applied to evaluate the statistical significance of the changes in spectral parameters (CIELAB coordinates and the projection of the

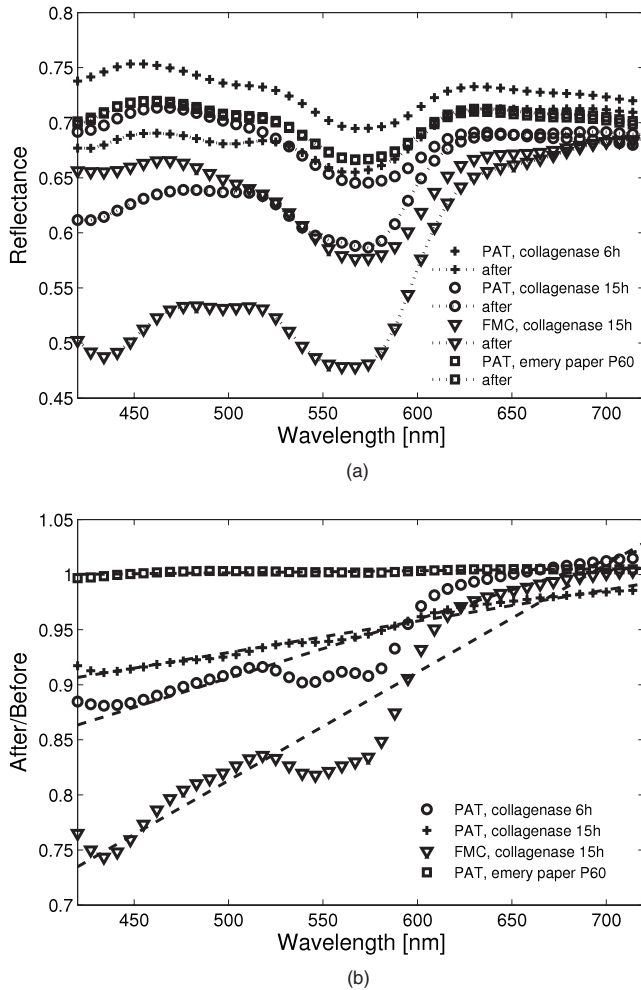


**Fig. 2** (a) Mean spectra and (b) the relative change at each wavelength before and after 6 h or 15 h collagenase digestion or mechanical grinding using the P60 emery paper for all the patellar (PAT) and femoral (FMC) samples. The dashed lines in (b) are the linear fits to the ratios of the two average spectra, before and after the treatments.

spectra to eigenvector) after experimental degradations were compared to initial situation before degradations. The Kruskal-Wallis *post hoc* test was used to reveal statistical differences in the spectral slope between the sample groups. The level of significance was set to  $p < 0.05$ . Statistical analyses were conducted using SPSS software (version 16.0, SPSS Inc., Chicago, Illinois).

### 3 Results

#### 3.1 Mean Reflectance Spectra

The mean reflectance spectrum at the center of each sample ( $200 \times 200$  pixels  $\approx 3.3 \times 3.3$  mm) was calculated before and after the degradation [Fig. 2(a)]. After collagenase digestion, the changes in the reflectance spectra were evident in the wavelengths up to 600 nm. However, in the wavelength range of 600 to 720 nm, the changes were only minor after collagenase digestion. In contrast, after mechanical degradation, no changes could be observed in the mean reflectance spectra.

A relative change after the experimental degradations is presented at each wavelength in Fig. 2(b). The mean slope (and the standard deviation) of the linear fit [Fig. 2(b)] in each sample group is presented in Table 1. The relative change is nearly linear after the 6 h collagenase digestion. After the 15-h digestion, some gaps in spectrum appear at wavelengths below 450 and around 550 nm, i.e., at the same spectral bands to maximal absorption of the hemoglobin.<sup>13</sup> The slopes after 15-h collagenase degradation are significantly different from those after mechanical degradation. After the 6-h collagenase degradation the slopes are significantly different only from the femoral samples (Table 1).

#### 3.2 CIELAB Color Coordinates

The CIELAB color coordinates were calculated for the samples at the center area ( $200 \times 200$  pixels). After enzymatic digestions, statistically significant ( $p < 0.05$ ) changes, depending on the immersion time and anatomical location, were observed in CIELAB coordinates (Table 2). Similarly as for the reflectance spectra, no significant changes in coordinates could be observed after the mechanical degradation.

**Table 1** The slope of the linear fit for the relative change between the mean wavelength dependent reflectances, before and after collagenase digestion (6 or 15 h) or mechanical degradation for the patellar (PAT) and femoral (FMC) samples.

	Slope (R / 100 nm)	6 h PAT (n=8)	15 h PAT (n=11)	15 h FMC (n=6)	Mechanical (n=7)
	Mean $\pm$ SD	0.0289 $\pm$ 0.0042	0.0533 $\pm$ 0.0103	0.0980 $\pm$ 0.0206	0.0018 $\pm$ 0.0031
$p$ value	6 h PAT	—	NS	0.003	NS
	15 h PAT	NS	—	NS	0.002
	15 h FMC	0.003	NS	—	0.001
	Mechanical	NS	0.002	0.001	—

The statistical significance (NS=nonsignificant) between the slopes is calculated by using the Kruskal-Wallis *post hoc* test.

**Table 2** Value of the CIELAB coordinates (mean $\pm$ SD) before and after mechanical degradation (mech.) and either 6- or 15-h enzymatic digestion using collagenase (coll.) for the patellar (PAT) and femoral medial condyle (FMC) samples. The *RGB* presentation of the colors and the  $\Delta E_{ab}^*$  color difference before and after treatments are also shown.

	PAT, coll. 6h.(n=8)		PAT, coll. 15h.(n=11)		FMC, coll. 15h(n=6)		PAT, mech. (n=7)	
	before	after	before	after	before	after	before	after
$L^*$	87.7 $\pm$ 1.0	85.8 $\pm$ 1.1 <sup>a</sup>	85.5 $\pm$ 1.0	82.8 $\pm$ 2.4 <sup>a</sup>	82.5 $\pm$ 1.5	77.4 $\pm$ 1.4 <sup>a</sup>	86.4 $\pm$ 1.6	86.4 $\pm$ 1.0
$a^*$	-0.1 $\pm$ 0.5	0.7 $\pm$ 0.4 <sup>a</sup>	0.0 $\pm$ 0.5	2.2 $\pm$ 1.0 <sup>a</sup>	1.9 $\pm$ 0.6	5.5 $\pm$ 0.8 <sup>a</sup>	0.1 $\pm$ 0.5	0.1 $\pm$ 0.5
$b^*$	-1.0 $\pm$ 1.0	0.7 $\pm$ 1.4 <sup>a</sup>	-1.5 $\pm$ 1.6	0.7 $\pm$ 2.6 <sup>a</sup>	-2.6 $\pm$ 0.4	2.7 $\pm$ 1.8 <sup>a</sup>	-0.6 $\pm$ 1.5	-0.6 $\pm$ 1.7
<i>RGB</i>								
$\Delta E_{ab}^*$	2.7		4.1		8.1		0.1	

<sup>a</sup>Statistically significant difference (Wilcoxon signed rank test,  $p < 0.05$ ) compared to sample before degradation.

The mean color difference  $\Delta E_{ab}^*$  showed that the color change after 15-h collagenase digestion was two times higher for the FMC than for the patella (Table 2).

### 3.3 PCA

The PCA was calculated for several subsets of the optical spectral image data. The sets for PCA, classified into groups by experimental treatments, were created by aggregating the spectra at the center area (200  $\times$  200 pixels) from all the samples with the same treatment. The spectra before and after degradation were taken separately and the PCA was calculated. The projections of spectral images to the second vector of the femoral samples after 15-h collagenase digestion were found to give good separation between the collagenase treatments and for the grinding marks caused by the emery paper (Fig. 3).

Figure 4 shows examples of the projection images. The projection shows uneven distribution of the spectral differences. The mean level of the center area (Fig. 5) in the

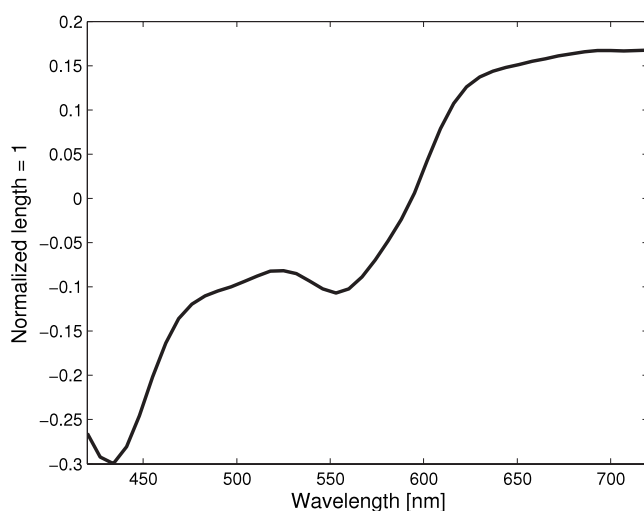


**Fig. 3** The second eigenvector after 15-h collagenase digestion of femoral samples. The projections of the cartilage spectra to the presented eigenvector were found to separate the enzymatic changes and emery paper scratches from the untreated samples. The vector was chosen to be the base vector for all the projections.

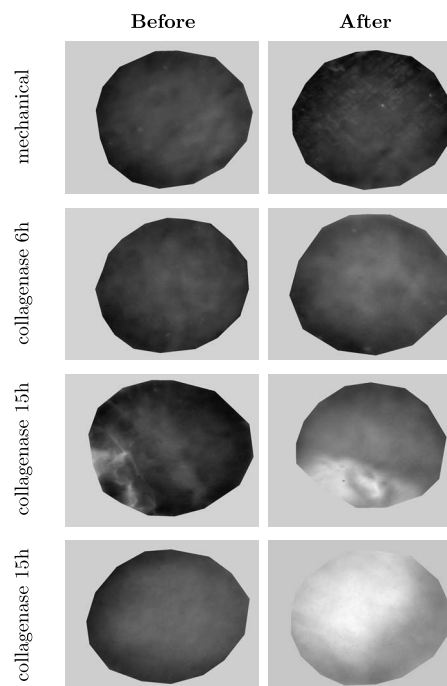


**Fig. 4** Examples of pseudocolor projections of the spectral images to the chosen base vector the second eigenvector of the femoral samples after 15-h collagenase digestion, Fig. 3. Representative patella (PAT) and femoral (FMC) samples before and after 6- or 15-h collagenase digestion or mechanical grinding using the P60 emery paper are shown. The PAT 15-h sample showed spontaneous trauma before collagenase digestion and is presented here for the purpose of comparison. All samples show clear spatial differences including the mechanical degradation marks (“scratches”) and the spontaneous trauma in the projection image before and after the collagenase digestion.

samples treated by the emery paper showed no statistically significant difference between the samples before and after the degradation. However, for enzymatic degradations the level increases when the immersion time is extended. The increase is significant ( $p < 0.05$ ) after all enzyme degradations.

In the characteristic images of the mechanically degraded sample (Fig. 6) the marks are faint in the visual appearance of the surface to the naked eye under the D65 illumination.<sup>†</sup> When using only one wavelength channel, the grinding is invisible at 700 nm. However, specifically at 469 nm the grinding can be seen. Use of one channel represents the case with the object viewed or illuminated through a narrow band filter. The projection of the sample spectra to the second eigenvector of FMC after 15-h enzyme treatment (Fig. 3) makes the grinding marks more visible in the cartilage and it was chosen to be the base vector for all the presented projections. The contrast calculation was performed for the 469-nm monochromatic and the projection image of the chosen base vector with the corresponding pixels. The contrast in projection image was found to be 1.6 to 2.5 times higher for each seven samples (Fig. 6). This kind of projection to the eigenvector indicates a combination of two images that are captured by using two separate complex optical filters.

<sup>†</sup>This is equal to the *RGB* presentation of the images.

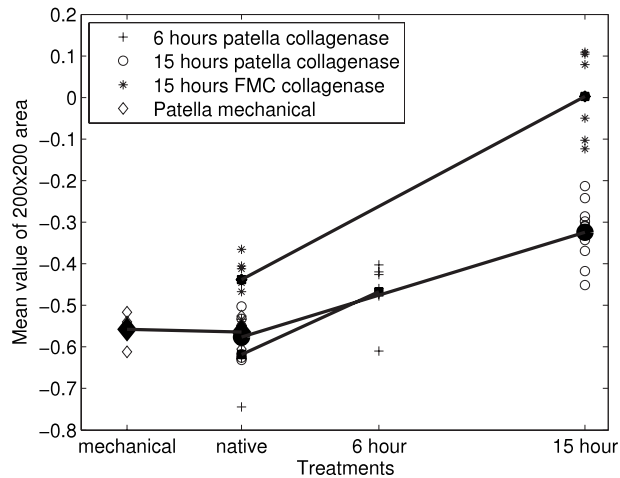


**Fig. 5** Mean values (200- $\times$ 200-pixel center area) of the projections of the spectral images to the chosen base vector (the second eigenvector of the femoral samples after 15-h collagenase digestion) for samples before and after enzymatic (6-/15-h collagenase) or mechanical degradations (P60 emery paper). The hollow circles indicate mean values within each sample, while the closed dots with lines represent the mean of samples within each group. The results from mechanical degradation are shown on the left side of the result of the native samples.

### 3.4 Optical Microscopy

One representative sample in each group was studied under a optical microscope. Further, cartilage thickness was evaluated from the microscopic images (Fig. 7). Mechanical degradation only affected the cartilage surface but the proteoglycan content, as assessed by safranin-O staining, was uniform, compared to that of collagenase digested samples. After the 6-h collagenase digestion, the proteoglycans were depleted from the superficial cartilage. The thickness of the mechanically degraded and 6-h collagenase-digested samples was typical of normal intact bovine patellar cartilage ( $1901 \pm 224 \mu\text{m}$ ) (see, e.g., Rieppo et al.<sup>20</sup>). In contrast, cartilage thickness was significantly reduced after the 15-h digestion with collagenase. Thickness of the one representative FMC sample was smaller (0.83 mm) than those of the patellar samples.

## 4 Discussion

In this study, the potential of visible light spectral imaging to quantify color changes in articular cartilage after experimental degradations, simulating OA, was investigated. Digestion by collagenase significantly changed the wavelength-dependent reflectance from the surface of bovine articular cartilage. The changes were more prominent at the shorter wavelengths, and statistically significant changes were observed for all the CIELAB coordinates.

The increase of the  $a^*$  coordinate, indicating an increase in the tissue “redness,” was probably contributed by the red color of the subchondral bone.<sup>11,13</sup> The characteristic absorption of the hemoglobin around 550 nm and below 450 nm (Ref. 13) was evident for samples after 15-h collagenase digestion (Fig. 2). A decrease in the lightness of the cartilage was related to the decrease in  $L^*$  coordinate. The changes in

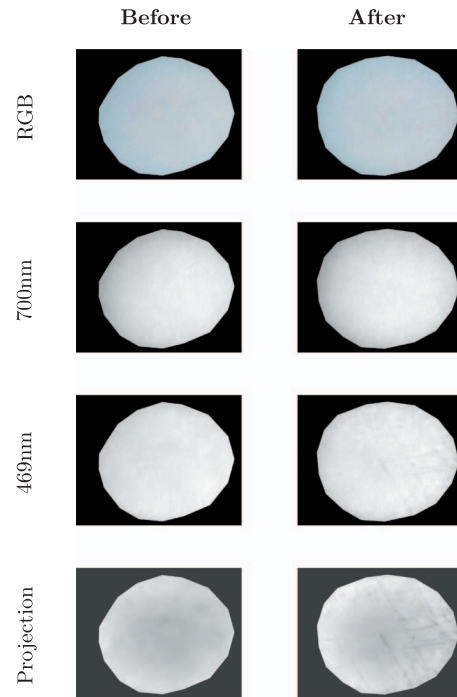


**Fig. 6** Examples of the visual appearance of one representative mechanically degraded cartilage sample in RGB, under monochromatic 700- and 469-nm light and after projection of spectra to the chosen base vector (the second eigenvector of the femoral samples after 15-h collagenase digestion). The mean contrast between the ground and intact areas in projection image is 1.6 to 2.5 timer higher for all the mechanically degraded samples when compared to image at 469 nm.

$L^*$  and  $a^*$  may be related to cartilage thickness. In the bovine knee joint, cartilage thickness at FMC is typically smaller than that in the patella.<sup>21</sup> Interestingly, the differences in  $L^*$  and  $a^*$  between the FMC and PAT cartilage are consistent with the changes of coordinates after 15-h collagenase digestion, characterized by reduction in cartilage thickness. The dependence of  $L^*$  and  $a^*$  on cartilage thickness is also supported by the finding that the coordinate values of FMC cartilage before digestion and PAT cartilage after digestion were nearly similar, matching with the equal cartilage thickness at those states.

Because of the degenerative nature of our treatments, assessment of the sample thickness before and after treatments

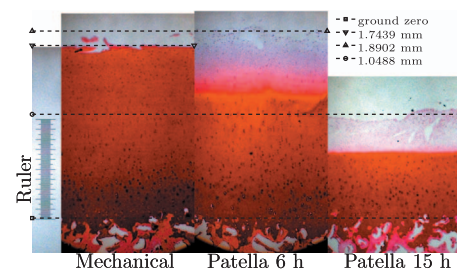


**Fig. 7** Optical microscopy images (safranin-O-stained sections) of the representative patellar samples after mechanical grinding with the P60 emery paper and after 6- and 15-h collagenase digestion. Cartilage thickness was determined from the captured images, calibrated by using the 1-mm ruler seen on the left.

was not feasible. As a limitation, we could determine the cartilage thickness for only one representative sample in each sample group. However, a statistically significant loss of bovine patella articular cartilage thickness after collagenase digestion, consistent with our findings, is reported by Wang et al.<sup>22</sup>

After 15-h collagenase digestion, the increase of the  $b^*$  coordinate from negative to positive values imply the color to transform from bluish to more yellow. Inconsistently with  $L^*$  and  $a^*$ , this change may not be explained by the variations in tissue thickness, but the changes in the  $b^*$  coordinate can be related to the cartilage structure, especially to those changes in the superficial zone of cartilage that could be revealed by the microscopy of the safranin-O stained tissue sections (Fig. 7). As cartilage is a complex tissue with multiple major components, such as collagen and proteoglycans, however, further studies should be conducted to reveal how the structural changes affect the spectrum.

In contrast, no significant changes in the mean optical reflectance spectrum were seen after mechanical degradation with the emery paper. However, by projecting the reflectance spectral image into carefully selected base vector (the second eigenvector of the femoral medial condyle data after the 15-h collagenase digestion) the visual appearance of the grinding marks after mechanical degradation was improved 1.6 to 2.5 times compared to the single channel image.

In this study, the same (native) samples before the treatments provided the control results for comparison with those after collagenase digestion and mechanical degradation. No separate control samples soaked for 6 or 15 h in PBS were included. This was accepted as in our previous study,<sup>20</sup> similar bovine patellar samples ( $n=12$ ) were soaked in PBS for 44 h with no significant differences in histological structure or composition, as judged by optical densitometry or polarized light microscopy. We strongly believe that the observed changes result from the collagen digestion or mechanical degradation.

Based on the studies by Ebert<sup>15</sup> and Qu et al.<sup>16</sup> the value of the scattering coefficient of intact cartilage tissue is of an order of magnitude larger than the absorption coefficient. Further, the tissue is highly forward scattering. The effect of collagenase digestion on the scattering in articular cartilage, to our knowledge, has not been studied. However, the discrete particle model by Schmitt and Kumar<sup>23</sup> indicates that the scatter-related attenuation depends on the ratio between the wavelength and the particle size in the tissue. When the collagen network is degraded by the collagenase and the proteoglycan content may also change (Fig. 7), the spectral differences (Fig. 2) may be attributed to a high concentration of collagen fragments that act as scattering centers. Thus, it seems that the spectral gaps below 450 and around 550 nm are more specific to advanced cartilage degeneration, i.e., when the thickness of the tissue is significantly reduced. Consequently, for diagnosis of early changes, more advanced spectral analysis methods may be necessary.

Significant correlation between the Mankin score and the Outerbridge classification with the  $L^*$  and  $a^*$  values of the CIELAB coordinate system was reported for human cartilage by Ishimoto et al.<sup>14</sup> They found a decrease in  $L^*$  coordinate and an increase in  $a^*$  along the progression of cartilage de-

generation. This is consistent with our findings on the effect of collagenase digestion. The increasing trend in the reflectance to the longer wavelengths in human cartilage samples differs from that found for the bovine cartilage in this study. The bovine reflectance from the intact sample showed nearly the same value at the both ends of the measured range. The differences between the reflectance spectra from human and bovine cartilage may arise from the differences in tissue thickness, as the human cartilage is known to be thicker than bovine cartilage.

While studying cartilage after microfracture repair, Hattori et al. have "hypothesized that the  $a^*$  value represents the color of the fibrin clot, while the  $L^*$  value indicates the newly formed cartilage"<sup>12</sup> in the repair tissue. Based on the presented spectral reflectance and color coordinate changes, this kind of generalization, however, should be done with caution.

All the earlier spectroscopic assessments of the articular cartilage<sup>11-14</sup> have been performed by measuring only a small surface area at the time. Because the degenerative changes in cartilage are highly dependent on the location, the actual state of the cartilage might not be reliably recorded with measurements at a small area. In this study, for the first time, the optical imaging approach was utilized and tested. We demonstrated that mechanical surface degradation with emery paper could only be revealed in imaging mode after sophisticated PCA algorithms. This algorithm could be used both for evaluating the collagenase-induced changes in cartilage and the grinding marks on the surface of the cartilage, i.e., increased surface roughness. Thus, imaging-based spectral measurements may provide more information on the cartilage integrity, and consequently may be recommended for further studies.

The presented techniques yielded good results for the bovine cartilage. However, they may not be optimized for human tissue. The development of an optimized algorithm for human cartilage is among our further aims. Importantly, the reflectance measurements and spectral imaging may be carried out with a fiber optic probe during diagnostic arthroscopies. Furthermore, optimal illuminations may be designed for arthroscopy to reveal sensitive and specific diagnostic information about the cartilage.

### Acknowledgments

The financial support from the Ministry of Education, Finland (University of Eastern Finland grant, Projects 5741/Kuopio and 10102/Joensuu), and from the Academy of Finland (Project 127198/Kuopio) is acknowledged.

### References

1. F. Guilak, A. Ratcliffe, N. Lane, M. P. Rosenwasser, and V. C. Mow, "Mechanical and biochemical changes in the superficial zone of articular cartilage in canine experimental osteoarthritis," *J. Orthop. Res.* **12**, 474-484 (1994).
2. J. P. Arokoski, J. S. Jurvelin, U. Väättäinen, and H. J. Helminen, "Normal and pathological adaptations of articular cartilage to joint loading," *Scand. J. Med. Sci. Sports* **10**(4), 186-198 (2000).
3. J. A. Buckwalter and H. J. Mankin, "Articular cartilage, part ii: degeneration and osteoarthritis, repair, regeneration, and transplantation," *J. Bone Joint Surg. Am.* **79**(4), 612-632 (1997).

4. X. Bi, X. Yang, M. P. Bostrom, and N. P. Camacho, "Fourier transform infrared imaging spectroscopy investigations in the pathogenesis and repair of cartilage," *Biochim. Biophys. Acta* **1758**(7), 934–941 (2006).
5. E. David-Vaudey, A. Burghardt, K. Keshari, A. Brouchet, M. Ries, and S. Majumdar, "Fourier transform infrared imaging of focal lesions in human osteoarthritic cartilage," *Eur. Cells Mater* **10**, 51–60 (2005).
6. H. Panula, M. Hyttinen, J. Arokoski, T. Langsjö, A. Pelttari, I. Kiviranta, and H. Helminen, "Articular cartilage superficial zone collagen birefringence reduced and cartilage thickness increased before surface fibrillation in experimental osteoarthritis," *Ann. Rheum. Dis.* **57**, 237–245 (1998).
7. X. Bi, G. Li, S. B. Doty, and N. P. Camacho, "A novel method for determination of collagen orientation in cartilage by fourier transform infrared imaging spectroscopy (FT-IRIS)," *Osteoarthritis Cartilage* **13**, 1050–1058 (2005).
8. S. Saarakkala, M. A. Laasanen, J. S. Jurvelin, and J. Töyräs, "Quantitative ultrasound imaging detects degenerative changes in articular cartilage surface and subchondral bone," *Phys. Med. Biol.* **51**, 5333–5346 (2006).
9. G. E. Kempson, C. J. Spivey, S. A. Swanson, and M. A. Freeman, "Patterns of cartilage stiffness on normal and degenerate human femoral heads," *J. Biomech.* **4**, 597–609 (1971).
10. C. G. Armstrong and V. C. Mow, "Variations in the intrinsic mechanical properties of human articular cartilage with age, degeneration, and water content," *J. Bone Joint Surg. Am.* **64**, 88–94 (1982).
11. K. Hattori, K. Uematsu, Y. Tanikake, T. Habata, Y. Tanaka, H. Yajima, and Y. Takakura, "Spectrocolorimetric assessment of cartilage plugs after autologous osteochondral grafting: correlations between color indices and histological findings in a rabbit model," *Arthritis Res. Ther.* **9**, R88 (2007).
12. K. Hattori, K. Uematsu, H. Matsumori, Y. Dohi, Y. Takakura, and H. Ohgushi, "Spectrocolorimetric evaluation of repaired articular cartilage after a microfracture," *BMC Res. Notes* **1**(1), 87 (2008).
13. P. Å. Öberg, T. Sundqvist, and A. Johansson, "Assessment of cartilage thickness utilising reflectance spectroscopy," *Med. Biol. Eng. Comput.* **42**, 3–8 (2004).
14. Y. Ishimoto, K. Hattori, H. Ohgushi, K. Uematsu, Y. Tanikake, Y. Tanaka, and Y. Takakura, "Spectrocolorimetric evaluation of human articular cartilage," *Osteoarthritis Cartilage* **17**(9), 1204–1208 (2009).
15. D. W. Ebert, "Articular cartilage optical properties in the spectral range 300–850 nm," *J. Biomed. Opt.* **3**(3), 326–333 (1998).
16. J. Qu, C. MacAulay, S. Lam, and B. Palcic, "Optical properties of normal and carcinomatous bronchial tissue," *Appl. Opt.* **33**(31), 7397–7405 (1994).
17. G. Wyszecki and W. S. Stiles, *Color Science*, 2nd ed., Wiley, New York (2000).
18. J. P. S. Parkkinen, J. Hallikainen, and T. Jääskeläinen, "Characteristic spectra of munsell colors," *J. Opt. Soc. Am. A* **6**, 318–322 (1989).
19. I. Kiviranta, J. Jurvelin, M. Tammi, A. M. Säämänen, and H. J. Helminen, "Microspectrophotometric quantitation of glycosaminoglycans in articular cartilage sections stained with safranin o," *Histochemistry* **82**(3), 249–255 (1985).
20. J. Rieppo, J. Töyräs, M. T. Nieminen, V. Kovanen, M. M. Hyttinen, R. K. Korhonen, J. S. Jurvelin, and H. J. Helminen, "Structure-function relationships in enzymatically modified articular cartilage," *Cells Tissues Organs* **175**(3), 121–132 (2003).
21. M. S. Laasanen, J. Töyräs, R. K. Korhonen, J. Rieppo, S. Saarakkala, M. T. Nieminen, J. Hirvonen, and J. S. Jurvelin, "Biomechanical properties of knee articular cartilage," *Biorheology* **40**(1–3), 133–140 (2003).
22. S. Wang, Y. Huang, S. Saarakkala, and Y. Zheng, "Quantitative assessment of articular cartilage with morphologic, acoustic and mechanical properties obtained using high-frequency ultrasound," *Ultrasound Med. Biol.* **36**, 512–527 (Mar. 2010).
23. J. M. Schmitt and G. Kumar, "Optical scattering properties of soft tissue: a discrete particle model," *Appl. Opt.* **37**(13), 2788–2797 (1998).